Journal of Chromatography A, 658 (1994) 149–171
Elsevier Science B.V., Amsterdam

CHROM. 25 156

Review

Modeling of preparative liquid chromatography

Sadroddin Golshan-Shirazi and Georges Guiochon*

Department of Chemistry, University of Tennessee, Knoxville, TN 37996-1501 (USA) and Division of Analytical Chemistry, Oak Ridge National Laboratory, Oak Ridge, TN 37831-6120 (USA)

ABSTRACT

In order to achieve an acceptable production rate at reasonable cost, preparative chromatography must be carried out with phase systems in which the kinetics of mass transfers and adsorption–desorption are fast. Accordingly, band profiles in overloaded chromatographic columns are best understood by considering the ideal model, while the process itself is most suitably modeled using the equilibrium-dispersive model. The former model assumes an infinite column efficiency, while the latter lumps the contributions of axial dispersion and mass transfer resistances into a single apparent dispersion coefficient. The properties and solutions of these models are reviewed. The conditions under which they give satisfactory results are summarized. The excellent agreement between the experimental band profiles of the components of binary mixtures and the individual band profiles calculated with the equilibrium-dispersive model is demonstrated. The degree of agreement is limited only by the accuracy with which the competitive equilibrium isotherms are accounted for.

CONTENTS

* Corresponding author. Address for correspondence: Department of Chemistry, University of Tennessee, Knoxville, TN 37996-1501, USA.

0021-9673/94/$26.00
SSDI 0021-9673(93)E0509-S

1. INTRODUCTION

In preparative chromatography, we need to produce significant amounts of purified compounds rather than information as in analytical chromatography. As a consequence, we cannot decouple simply the thermodynamics of the retention mechanism and the kinetics of mass transfers in the column. We also cannot consider the mixture components separately. We have to consider the elution of the whole mixture as a single problem and handle all aspects of the problem at the same time, including the kinetics and thermodynamics of phase equilibria. Thus, in the general case, preparative chromatography is a most complex phenomenon to model.

The fundamental approach to this problem, then, consists in writing the differential mass balance equations for all the mixture components, and considering simultaneously the two aspects of the problem: (i) the thermodynamics of phase equilibrium, or the distribution of the mixture components between the mobile and the stationary phases; and (ii) the kinetics of phase transfers, *i.e.*, the combined effects of the axial dispersion, the mass transfer resistances (including the external fluid film resistance and the intraparticle diffusion) and the finite kinetics of the adsorption–desorption.

We have just summarized the features of the general rate model of chromatography. An analytical solution of this model is available in linear chromatography [1]. This is possible because, if we assume a linear isotherm, the problem reduces to that of a single component, and the mass balance equation simplifies considerably. In preparative chromatography, extreme complexity arises, as noted above, from (i) the non-linearity of isotherms, (ii) the coupling of the mass balance equations of the different components due to the dependence of the equilibrium isotherm of each component on the mobile phase concentration of the other components, (iii) the coupling of the kinetics of mass transfers of the different components due to the influence of each on the mass transfer kinetics of all the others and (iv) the coupling between the thermodynamic and the kinetic effects. As a result of this complexity, a solution of the general rate model with non-linear isotherms can be achieved only by the use of a numerical method [2,3]. Such a solution is complex and requires sophisticated programming and long CPU times. Further, it requires the availability of a large number of coefficients which are often difficult to estimate and almost impossible to measure independently of the chromatographic process. Fortunately, it appears that all the information required for the development and/or the study of the chromatographic process for preparative applications on an industrial scale can be obtained in most instances with simpler models.

A considerable simplification of the model with negligible loss of accuracy can be achieved by making some simple assumptions. Two much simpler models are available. In the ideal model, we neglect the influence of the mass transfer resistances, and assume plug flow (*i.e.*, neglect the axial dispersion). The ideal model gives the output response of a column having an infinite efficiency. Thus, this model tells us what the thermodynamics of phase equilibria tries to accomplish, and what it permits. In the equilibrium-dispersive model, we still assume constant

equilibrium between the mobile and the stationary phases, but we lump the finite rate of mass transfer and the axial dispersion into an apparent axial dispersion coefficient. This last model gives results that are in nearly perfect agreement with experimental results. The reasons for this are (i) the overwhelming influence of the thermodynamics of equilibrium on the band profiles at high concentrations, making the influence of kinetics a mere correction, and (ii) the availability of stationary phases that afford fast kinetics of mass transfer and adsorption–desorption.

Accordingly, this review will deal only with the ideal and the equilibrium-dispersive models of chromatography. We present these models, describe their main features and properties, discuss their solutions and discuss the degree of agreement with experimental results.

2. THE IDEAL MODEL

In the ideal model, we ignore the axial dispersion and the kinetics of mass transfer. Thus, the column efficiency is assumed to be infinite. The ideal model has been developed by Wilson [4]. Important contributions to its solutions have been made by DeVault [5], Offord and Weiss [6], Glueckauf [7,8], Rhee *et al.* [9], Helfferich and Klein [10], Guiochon and Jacob [11] and Golshan-Shirazi and Guiochon [12,13].

The differential mass balance equation for each component can be written as [4]

$$u \cdot \frac{\partial C_i}{\partial z} + \frac{\partial C_i}{\partial t} + F \cdot \frac{\partial q_i}{\partial t} = 0 \tag{1}$$

where C_i and q_i are the concentrations of component i in the mobile and the stationary phases, respectively, z and t are the position and time, respectively, u is the mobile phase linear velocity, $F = v_s/v_m = (1-\epsilon)/\epsilon$ is the phase ratio and ϵ is the total porosity of the packed column; q_i and C_i are related through the equilibrium isotherm:

$$q_i = f(C_1, C_2, \ldots, C_i, \ldots, C_n) \tag{2}$$

As noted above, it is the non-linear behavior of the isotherm which plays the major role in shaping the elution profile. This justifies the use of the ideal model and explains why it gives a good caricature of what is happening during the migration of the component bands, and how the final chromatogram is evolving.

Finally, to solve a partial differential equation, we need initial and boundary conditions. In overloaded elution, the column is empty of sample at the beginning of the experiment, and in equilibrium with the pure mobile phase. The initial condition is given by

$$C_i(0, z) = 0 \tag{3}$$

We assume that the sample is introduced into the column as a pulse injection. The corresponding boundary condition is

$$C_i(t, 0) = C_{i,0} \quad 0 \leq t \leq t_p \tag{4a}$$

$$C_i(t, 0) = 0 \quad t > t_p \tag{4b}$$

We describe first the main feature of the ideal model before giving its general solution.

2.1. Solution of the ideal model for a single component

Eqn. 1 can be rewritten as

$$\frac{\partial C}{\partial t} + \frac{u}{1 + F \cdot \dfrac{dq}{dC}} \cdot \frac{\partial C}{\partial z} = 0 \tag{5}$$

This equation shows that a velocity can be associated with each concentration. This velocity is given by

$$u_z = \frac{u}{1 + F \cdot \dfrac{dq}{dC}} \tag{6}$$

If we have a convex upwards isotherm, the concentration in the stationary phase at equilibrium increases less rapidly than the concentration in the mobile phase, $d^2q/dC^2 < 0$, and the velocity associated with a concentration C increases with increasing concentration. The real or diffuse boundary of the elution profile spreads progressively, as the band maximum moves faster than the limit point at infinite dilution. This point, the last one of the band profile, moves at the velocity $u = u_0/(1 + k'_0)$ observed under analytical conditions (with $k'_0 = Fa$, where a is the slope of the isotherm at the origin).

In the front of the band we have a problem, however, which arises from the fact that as the high concentrations move faster than the low concentrations, the band maximum tries to pass the band beginning, at $C = 0$. This is impossible, and it can be shown that all the concentrations will pile up at the same time. One of the properties of eqn. 1 is its ability to propagate concentration discontinuities or shocks. The shock velocity is given by

$$U_s = \frac{u}{1 + F \cdot \frac{\Delta q}{\Delta C}} \tag{7}$$

where Δq and ΔC are the differences between the concentrations at the front and the rear of the shock in the mobile and the stationary phase, respectively.

2.2. General solution of the ideal model for a single component

It results from eqn. 6 that the diffuse boundary of a convex upwards isotherm is given by

$$t(C) = t_p + \frac{L}{u}\left(1 + F \cdot \frac{dq}{dC}\right) \tag{8}$$

where $t(C)$ is the retention time of the concentration C at the end of a column of length L. If the isotherm is convex upwards, $t(C)$ increases with decreasing C, and the diffuse boundary is a rear profile. The converse is true for a convex downward isotherm.

In the case of a single component, for any isotherm which has no inflection point, the retention time of the concentration discontinuity with the initial and boundary conditions of eqns. 3 and 4 is given by [8,13]

$$\left| q(C_M) - C_M \cdot \frac{dq}{dC} \right|_{C=C_M} = \frac{n}{F_v t_0 F} \tag{9}$$

where n is the amount of compound injected (number of moles), F_v is the volume flow-rate of the mobile phase and t_0 is the column hold-up time. Depending on the isotherm equation, it is possible to derive an analytical or a numerical solution of eqn. 9.

2.3. Case of the Langmuir isotherm

The equation of the Langmuir isotherm is

$$q = \frac{aC}{1 + bC} \tag{10}$$

where a and b are numerical coefficients. This isotherm is convex upwards. The elution profile [13,14] begins with a shock at

$$t_R = t_p + t_0 + (t_{R,0} - t_0)(1 - \sqrt{L_f})^2 \tag{11}$$

where $t_{R,0}$ is the retention time under analytical (*e.g.*, linear) conditions:

$$t_{R,0} = t_0(1 + Fa) = t_0(1 + k'_0) \tag{12}$$

and L_f is the loading factor, or ratio of the sample size and the column saturation capacity:

$$L_f = \frac{nb}{\epsilon S L k'_0} \tag{13}$$

At the top of the shock begins the rear, diffuse boundary with an equation

$$C = \frac{1}{b}\left[\sqrt{\frac{t_{R,0} - t_0}{t - t_p - t_0}} - 1\right] \tag{14}$$

The maximum concentration, at the top of the shock, is

$$C_M = \frac{\sqrt{L_f}}{b(1 - \sqrt{L_f})} \tag{15}$$

The band ends at

$$t_R(0) = t_p + t_{R,0} \tag{16}$$

These equations define entirely the solution. We note that the profile (eqn. 14) can be normalized by using as reduced coordinates $k' = (t - t_p - t_0)/(t_{R,0} - t_0)$ and bC.

2.4. Case of the biLangmuir isotherm

The biLangmuir isotherm equation is

$$q = \frac{a_1 C}{1 + b_1 C} + \frac{a_2 C}{1 + b_2 C} \tag{17}$$

This equation corresponds to a heterogeneous surface, paved with two different types of sites, and can be used, for example, for polar com-

pounds on chemically bonded reversed phases. In this case, the solution [13] is made of a diffuse rear boundary given by

$$t_R(C) = t_p + t_0 + Ft_0 \cdot \frac{a_1(1+b_2C)^2 + a_2(1+b_1C)^2}{[1+(b_1+b_2)C+b_1b_2C^2]^2} \quad (18)$$

This bands ends at

$$t_R(0) = t_p + t_0[1 + F(a_1 + a_2)] \quad (19)$$

and starts at a time which can be calculated by numerical solution of the algebraic equation

$$\left| \int_{t_R}^{t_{R,0}} + t_p C \, dt \right| = \frac{n}{F_v} \quad (20)$$

using eqn. 18, which relates C and t.

2.5. Comparison with experimental results

As we have assumed an infinitely efficient column, we could expect poor agreement between the band profiles just calculated and those recorded in experiments performed with high-concentration bands of pure compounds. However, when the adsorption behavior of these compounds is described accurately by a known isotherm, the experiment band profiles agree well with those derived from eqns. 8 and 9. The reason for such good agreement is that thermodynamics play the major role in shaping the band profile at high concentrations.

For example, Fig. 1 shows the experimental profiles recorded with phenol on a C_{18} chemically bonded column, and the profiles calculated with the ideal model for column loadings increasing from 2 to 11% [15]. In Fig. 2, we compare the profiles of bands of benzyl alcohol in normal-phase chromatography, for values of the column loading factor increasing from 0.15 to 6%. In all instances, the actual band fronts are not truly vertical as predicted. They are very steep, however, and the difference in the front slope from vertical is really significant only for the smallest peak. It becomes truly negligible for the largest peaks. The rear part of the profile of the actual band is more strongly curved than the predicted profile and it tails longer. The influences of the

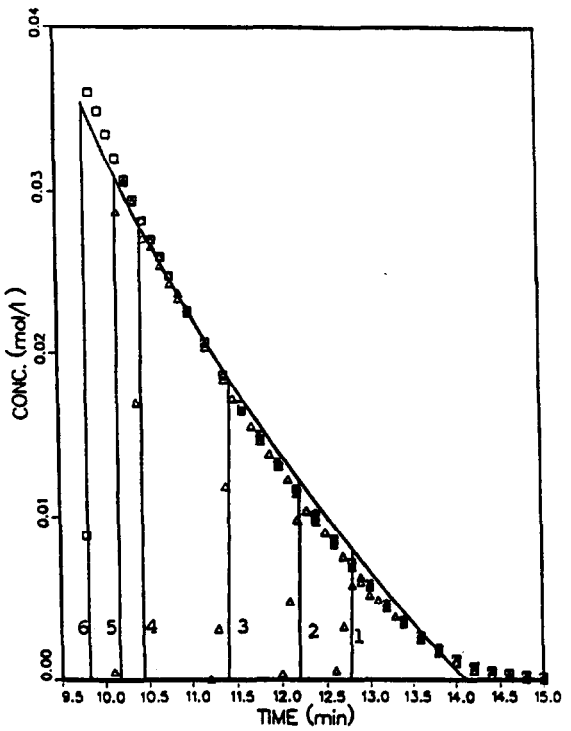

Fig. 1. Comparison of the experimental band profiles and the profiles calculated with the ideal model for phenol on C_{18}-bonded silica, eluted with methanol–water (20:80). Flow-rate, 1 ml/min. Sample loading factors (size in mmol); 2.1 (0.015), 4.3 (0.03), 6.4 (0.045), 8.5 (0.06) and 10.7% (0.075). From ref. 15 (© American Chemical Society).

axial dispersion and the finite rate of the mass transfers in the column, which we have neglected, easily explain these differences. An experimental band profile may have steep front and a tailing rear. It cannot have a vertical front. The concentration gradient would be infinite and generate an infinite mass flux. The solutes cannot diffuse instantaneously to the core of the packing particles.

3. MULTI-COMPONENT IDEAL CHROMATOGRAPHY

Glueckauf [7] was the first to give a solution of the ideal model of chromatography for overloaded elution and displacement chromatograpy, in the case of a binary mixture of compounds following the competitive Langmuir isotherm model. A comprehensive theoretical study of the

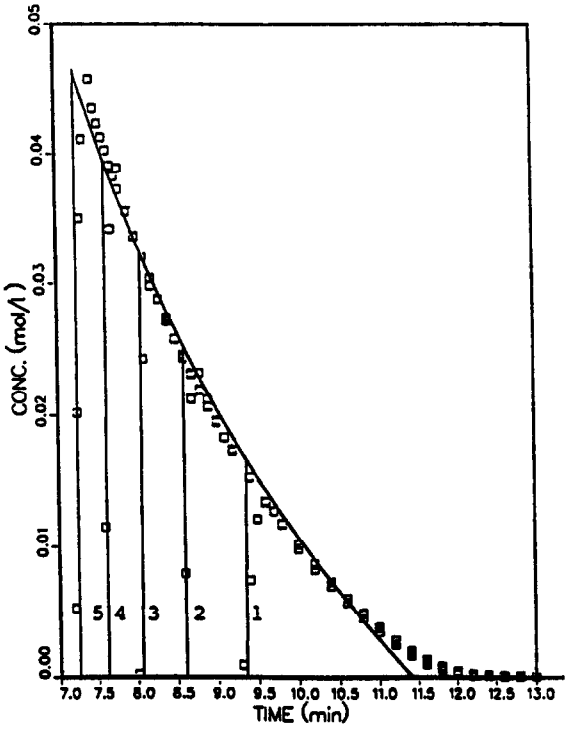

Fig. 2. Comparison of the experimental band profiles and the profiles calculated with the ideal model for benzyl alcohol on silica, eluted with THF–*n*-heptane (15:85). Flow-rate, 1 ml/min. Sample loading factor (sample size in mmol): 0.47 (0.00625), 0.95 (0.0125), 1.9 (0.025), 3.8 (0.050), 4.6 (0.060) and 5.7% (0.075). From ref. 15 (© American Chemical Society).

multi-component problem in ideal chromatography was given by Rhee *et al.* [9]. They developed the simple waves and the shock waves theories, illustrated their results by analyzing wave interactions and constructed the solutions. Their theory can be applied to the solution of problems of frontal analysis, overloaded elution and displacement chromatography. Helfferich and Klein [10] made another theoretical analysis of multi-component ion-exchange chromatography using the ideal model and employing the *h*-transform and the concept of coherence. This theory is mainly applied in displacement chromatography, although it can be used also in overloaded elution [10,16]. None of these papers contain a detailed description of the analytical solution and a simple calculation procedure to derive it from given values of the isotherm parameters. These data were given with a solution of the problem of the overloaded elution of two compounds, assuming the ideal model and competitive Langmuir isotherms [12,16]. This solution can be derived using either the method of characteristics [17] or the *h*-transform [10].

3.1. General properties of the equation system for two components with competitive Langmuir isotherms

In the case of a binary mixture, we need to write two differential mass balance equations, one for each compound:

$$\frac{\partial C_1}{\partial t} + F \cdot \frac{\partial q_1}{\partial t} + u \cdot \frac{\partial C_1}{\partial z} = 0 \tag{21a}$$

$$\frac{\partial C_2}{\partial t} + F \cdot \frac{\partial q_2}{\partial t} + u \cdot \frac{\partial C_2}{\partial z} = 0 \tag{21b}$$

The competitive Langmuir isotherms of the two components are given by

$$q_1 = \frac{q_{s,1} b_1 C_1}{1 + b_1 C_1 + b_2 C_2} \tag{22a}$$

$$q_2 = \frac{q_{s,2} b_2 C_2}{1 + b_1 C_1 + b_2 C_2} \tag{22b}$$

In the case of a binary mixture, there are two sets of equations describing the velocities associated with the concentrations C_1 and C_2 and the shock velocities, respectively. These equations are similar to eqns. 6 and 7 for a single component, respectively. The velocity associated with given concentrations of the two compounds on a diffuse boundary of the individual profiles is given by

$$u_{z,1} = \frac{u_0}{1 + F \cdot \dfrac{Dq_1}{DC_1}} \tag{23a}$$

$$u_{z,2} = \frac{u_0}{1 + F \cdot \dfrac{Dq_2}{DC_2}} \tag{23b}$$

where the term Dq_i/DC_i is given by

$$\frac{Dq_1}{DC_1} = \frac{\partial q_1}{\partial C_1} + \frac{dC_2}{dC_1} \frac{\partial q_1}{\partial C_2} \tag{24a}$$

$$\frac{Dq_2}{DC_2} = \frac{\partial q_2}{\partial C_2} + \frac{dC_1}{dC_2}\frac{\partial q_2}{\partial C_1} \quad (24b)$$

The velocities of the concentration shocks of the two components are

$$U_{s,1} = \frac{u_0}{1 + F\left(\frac{\Delta q_1}{\Delta C_1}\right)} \quad (25a)$$

$$U_{s,2} = \frac{u_0}{1 + F\left(\frac{\Delta q_2}{\Delta C_2}\right)} \quad (25b)$$

The most important property of the directional differentials given in eqns. 24a and 24b is that they are equal (coherence condition). Thus, the velocities $u_{z,1}$ and $u_{z,2}$ associated with the two components in the continuous parts of the profiles are also equal:

$$u_{z,1} = u_{z,2} = u_z \quad (26)$$

This relationship, which was first suggested by Offord and Weiss [6], is necessary to obtain the analytical solution of the system of eqns. 21. The coherence condition of Helfferich [10] is a concept equivalent to this relationship.

Using eqns. 23a, 23b, 24a and 24b, and letting $r = dC_1/dC_2$, one can derive from eqn. 26 that

$$\frac{\partial q_2}{\partial C_1} \cdot r^2 + \left(\frac{\partial q_2}{\partial C_2} - \frac{\partial q_1}{\partial C_1}\right)r - \frac{\partial q_1}{\partial C_2} = 0 \quad (27)$$

For Langmuir competitive isotherms, we can calculate the derivatives of eqns. 22a and 22b, insert these values into eqn. 27 and, letting $\alpha = a_2/a_1 = k'_2/k'_i$, we obtain the equation:

$$\alpha b_1 C_2 r^2 - (\alpha - 1 + \alpha b_1 C_1 - b_2 C_2)r - b_2 C_1 = 0 \quad (28)$$

As long as the plateau concentration of the wide rectangular injection pulse has not eroded away completely, we have $C_1 = C_1^0$ and $C_2 = C_2^0$ in eqn. 28. This equation becomes in this instance

$$\alpha b_1 C_2^0 r^2 - (\alpha - 1 + \alpha b_1 C_1^0 - b_2 C_2^0)r - b_2 C_1^0 = 0 \quad (29)$$

Using the equations just discussed, it is possible to derive the analytical solution of the system of eqns. 21 in the case of Langmuir competitive isotherms. This solution consists of three zones. The first zone contains only the first (or less retained component), the second (or mixed) zone contains both components and the third zone contains only the second (or more retained component), as illustrated in Fig. 3a and b.

Fig. 3a shows a typical solution of the two-component problem in a case where complete resolution is not achieved. Fig. 3b shows the hodograph transform of the solution in Fig. 3a. This transform is obtained by plotting the concentration of the first component, C_1, *versus* that of the second component, C_2, at the same time during the elution of the band. It can be shown that this plot gives two lines, one for the band front and the other for the rear, and that these two lines are straight in the case of competitive Langmuir isotherms.

In the case of a wide rectangular injection, wide enough for part of the injection plateau to elute without being eroded away, the roots of eqn. 29 are the slopes of the two lines in the hodograph plane emanating from the point representing the composition of the feed injection (C_1^0, C_2^0, point F in Fig. 3b). The positive root is the slope of the straight line corresponding to the pathway of the continuous part of the profiles in the mixed zone. The negative root corresponds to the shock between the first and second (mixed) zones.

3.2. Rear diffuse boundaries of the elution profiles in the case of a wide injection

The solution is particularly simple, because we have a constant state, corresponding to what is left of the injection plateau, and a simple wave solution. The straight line with a positive slope in Fig. 3b intersects the C_2 axis at point B, with the concentration

$$C_2^B = C_2^0 - \frac{C_1^0}{r_1} \quad (30a)$$

The value of the second term in the right-hand side of eqn. 30a can be obtained from 29:

$$C_2^0 - \frac{C_1^0}{r_1} = \frac{\alpha - 1}{\alpha b_1 r_1 + b_2} \quad (30b)$$

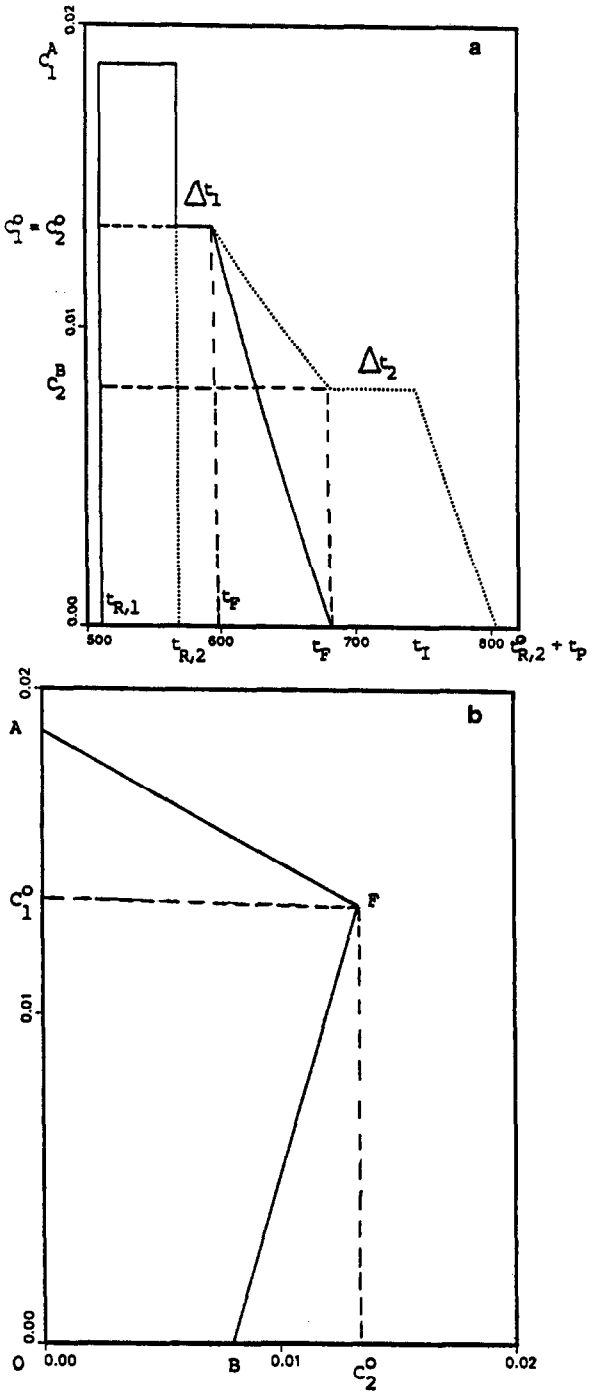

Fig. 3. Solution of the ideal model for a wide rectangular pulse injection of a 1:1 mixture. (a) Elution profile of a wide rectangular injection, showing the various characteristic points of the solution (see equations in text). The solid line gives the band profile of the first component and the dotted line that of the second component. (b) Hodograph transform of the profiles in (a).

The concentrations C_1 and C_2 in the mixed zone are not independent, but are related according to

$$C_2 - \frac{C_1}{r} = \frac{\alpha - 1}{\alpha b_1 r_1 + b_2} \tag{31}$$

The velocity associated with a pair of concentrations C_1 and C_2 on the continuous parts of the profile in the mixed zone can be obtained from eqns. 23a and 24a, using the derivatives of the isotherm (eqn. 22):

$$u_z = \frac{u}{1 + \dfrac{Fa_1\left[1 + b_2\left(C_2 - \dfrac{C_1}{r_1}\right)\right]}{(1 + b_1 C_2 + b_2 C_2)^2}} \tag{32}$$

The combination of eqns. 31 and 32 (considering that $t = t_p + z/u_z$) gives the continuous part of the band profiles of the two components in the mixed zone [12]:

$$C_1 = \frac{1}{b_1 + b_2/(\alpha r_1)}\left[\sqrt{\frac{\gamma}{\alpha}\cdot\frac{t^0_{R,1} - t_0}{t - t_p - t_0}} - 1\right]$$

$$\text{with} \quad 0 < C_1 < C_1^0 \tag{33a}$$

$$C_2 = \frac{1}{b_2 + \alpha b_1 r_1}\left[\sqrt{\gamma\cdot\frac{t^0_{R,2} - t_0}{t - t_p - t_0}} - 1\right]$$

$$\text{with} \quad 0 < C_2 < C_2^0 \tag{33b}$$

where, to simplify the writing of these equations, we have let $\gamma = (\alpha b_1 r_1 - b_2)/(b_1 r_1 + b_2)$. We can obtain the time when the mixed zone ends by inserting $C_1 = 0$ into eqn. 33a or $C_2 = C_B$ into eqn. 33b:

$$t_E = t_p + t_0 + \frac{\gamma}{\alpha}(t^0_{R,1} - t_0) = t_p + t_0\left(1 + \frac{\gamma Fa_1}{\alpha}\right) \tag{34}$$

The continuous part of the band profile in the third zone of the chromatogram (where the second component is pure), corresponding to the region OB in Fig. 3b, is obtained from eqn. 14:

$$C_2 = \frac{1}{b_2}\left[\sqrt{\frac{t^0_{R,2} - t_0}{t - t_p - t_0}} - 1\right] \tag{35}$$

The time when the concentration of the second

component in the third zone reaches C_2^B is given by

$$t_I = t_p + t_0\left[1 + Fa_2\left(\frac{\gamma}{\alpha}\right)^2\right] = t_p + t_0\left[1 + Fa_1\left(\frac{\gamma^2}{\alpha}\right)\right] \quad (36)$$

By comparing eqns. 34 and 36, and since γ is always greater than 1, we find that t_E is always shorter than t_I, so a plateau with a constant concentration equal to C_2^B appears at the beginning of the third zone, or elution zone of the pure component 2. The length of this plateau is given by

$$\Delta t = t_I - t_E = \frac{\gamma Fa_1}{\alpha}(\gamma - 1)t_0 \quad (37)$$

In the case of a wide rectangular band, the time when the injection plateau ends and the rear diffuse boundaries of both component profiles begin can be obtained by inserting $C_1 = C_1^0$ in eqn. 33a or $C_2 = C_2^0$ in eqn. 33b. We obtain

$$t_F = t_p + t_0\left[1 + \frac{Fa_2}{\gamma(1 + b_1C_1^0 + b_2C_2^0)^2}\right] \quad (38)$$

3.3. Front shocks in the case of a wide injection

The negative root of eqn. 29 is the slope of the line that represents the second shock of the profile, between the first and second zones. This line intersects the C_1 axis at point A, with the concentration

$$C_1^A = C_1^0 - r_2C_2^0 \quad (39)$$

Hence, immediately after the injection begins, two shocks are formed in the band front. The first shock is at the front of the first component band. According to eqn. 25a, its velocity is

$$U_{s,OA} = \frac{u}{1 + F \cdot \dfrac{a_1}{1 + b_1C_1^A}} \quad (40)$$

A second shock is formed between the first and second zones, at the front of the second component band. Its velocity is given by eqn. 25b:

$$U_{s,FA} = \frac{u}{1 + F \cdot \dfrac{a_2}{1 + b_1C_1^0 + b_2C_2^0}} \quad (41)$$

The first zone, located between these two shocks, contains only the pure first component. As long as the plateau of the injected pulse corresponding to point F in the Fig. 3b has not been eroded away, the velocities of these two shocks remain constant. Then, it is easy to derive the analytical solution giving their retention times from their constant velocities, in eqns. 40 and 41. Considering that $t_{R,1} = z/U_{s,FA}$ and $t_{R,2} = z/U_{s,FA}$ [12], we have at the column end ($z = L$)

$$t_{R,1} = t_0\left(1 + \frac{Fa_1}{1 + b_1C_1^A}\right) \quad (42)$$

$$t_{R,2} = t_0\left(1 + \frac{Fa_2}{1 + b_1C_1^0 + b_2C_2^0}\right) \quad (43)$$

3.4. Case of a narrow rectangular injection pulse

A narrow injection pulse is defined as a rectangular injection pulse for which the injection plateau is eroded and disappears at an intermediate stage of the migration. The injection plateau disappears just when the band is eluted if

$$t_{R,2} = t_F \quad (44)$$

where $t_{R,2}$ is given by eqn. 43 and t_F by eqn. 38. If $t_{R,2} < t_F$, we have a "wide" injection band, and a plateau at the injection concentration is part of the elution profile. In contrast, if $t_{R,2} > t_F$, we have a "narrow" injection band and the plateau erodes and disappears. When this happens, the shock velocities no longer remain constant. They depend on the differences between the component concentrations on both sides of the shock, and these concentrations decrease.

Nevertheless, an analysis of the interactions between simple waves and shock waves permits the derivation of the analytical solution (i) for the retention time of the second shock, (ii) for the continuous band profiles of the first component between the two shocks and after the second shock and (iii) for the continuous band profiles of the second component after the second shock. However, the retention time of the first component can be obtained only by the numerical integration of the area of the first

component band profile, which must remain equal to the injected area of that component [12].

Table 1 gives a summary of the analytical results corresponding to the different zones.

3.5. Comparison between the profiles predicted by the ideal model for a binary mixture and experimental results

No detailed comparisons made in this case are available. However, systematic comparisons have been made between the band profiles calculated with the ideal and the equilibrium-dispersive model (see next section). As this later model compares extremely well with the experimental results, this study answers the question. At high loading factors, there is a small difference between the experimental profiles and those predicted by the ideal model. As expected, and as observed in the single-component case, the only significant differences are the erosion of the concentration shocks, providing steep but not vertical concentration fronts, and in the rear plateau on the second component band, at the beginning of the third zone. Unless the concentration of the first component far exceeds that of the second, this plateau is eroded, and only an inflection point can be seen.

4. EQUILIBRIUM-DISPERSIVE MODEL OF CHROMATOGRAPHY

The ideal model of chromatography, which assumes a column with infinite efficiency, gives a reasonable caricature of the elution profiles when the column efficiency and the loading factor are high. An analytical solution is obtained in the case of the competitive Langmuir model only for a binary mixture. However, we have seen that kinetic effects smooth the band profiles obtained with real columns. The shocks are replaced by steep boundaries with a finite thickness, *i.e.*, by shock layers, plateaux are eroded and the band profiles end later than predicted by the ideal model. Further, in many instances, the competitive Langmuir model is inapplicable.

A more realistic model should include the effects of a finite column efficiency, *i.e.*, should take into account the contributions of the axial dispersion and the mass transfer resistances. In the equilibrium-dispersive model of chromatography, we assume that the components are in constant equilibrium between the mobile and the stationary phases and that all the contributions to band broadening can be lumped into a single apparent dispersion coefficient. Hence the mass balance equation in this model is given by

$$u \cdot \frac{\partial C_i}{\partial z} + \frac{\partial C_i}{\partial t} + F \cdot \frac{\partial q_i}{\partial t} = D_{a,i} \cdot \frac{\partial^2 C_i}{\partial z^2} \qquad i = 1, n \tag{45a}$$

where $D_{a,i}$ is an apparent dispersion coefficient related to the column HETP. For a single component, we have

$$D_a = \frac{Hu}{2} \tag{45b}$$

We have shown [1] that, in linear chromatography, all the kinetic models used to account for the various kinetic phenomena involved in a chromatographic column give the same results, equivalent to the Gaussian band profile predicted by the plate theory, even when the efficiency is as low as 100 theoretical plates. The models studied include (i) the general rate model, (ii) the pore model, (iii) the linear driving force model and (iv) the equilibrium dispersive model [1]. In linear chromatography, the variances of the contributions of the various sources of band broadening are additive [18] and the models give the same results. Thus, the equilibrium-dispersive model gives the exact solution for the band profile. However, we are interested here in the problem of overloaded elution and the variances of shift-variant contributions are no longer additive [19].

4.1. Reduction of the kinetic models to the equilibrium-dispersive model

Rhee and Amundson [20] have discussed the additivity of the contributions due to axial dispersion and to the mass transfer kinetics in nonlinear chromatography. They have also studied the properties of shock layers in the case of a

TABLE 1

EQUATIONS DESCRIBING THE SOLUTION OF THE IDEAL MODEL FOR TWO COMPONENTS WITH LANGMUIR COMPETITIVE ISOTHERMS AND A NARROW RECTANGULAR PULSE INJECTION

First zone: pure first component

Retention time of the first component: this retention time cannot be calculated in closed form. It is obtained as the lower boundary of the finite integral of the two profiles of the first component (in the first and second zones), such that this integral be equal to the area of the injected profile, *i.e.*, corresponds to the mass of first component injected.

Concentration profile of the first component:

$$t = t_p + t_0 + (t^0_{R,1} - t_0)\left\{\frac{1}{(1+b_1C_1)^2} - L_{f,2}\cdot\frac{\alpha-1}{\alpha}\cdot\frac{1}{[(\alpha-1)/\alpha + b_1C_1]^2}\right\}$$

Concentration of the first component on the front side of the second shock:

$$C_1^{A'} = \frac{1}{b_1}\cdot\frac{(1-\alpha)/\alpha + \sqrt{L'_f}}{1-\sqrt{L'_f}}$$

with

$$L'_f = \left(1 + \frac{b_1 r_1}{b_2}\right)L_{f,2}$$

where $L_{f,2}$ is the loading factor for the second component:

$$L_{f,2} = \frac{n_2 b_2}{\epsilon S L k'^0_2} = \frac{b_2 C^0_2 t_p}{t^0_{R,2} - t_0}$$

Mixed zone

Retention time of the second shock:

$$t_{R,2} = t_p + t_0[1 + Fa_2\gamma(1-\sqrt{L'_f})^2]$$

Concentration of the first component on the rear side of the second shock:

$$C_1^M = \frac{r_1}{b_2 + \alpha b_1 r_1}\cdot\frac{1-\alpha+\alpha\sqrt{L'_f}}{1-\sqrt{L'_f}}$$

Concentration of the second component at the top of the second shock:

$$C_2^M = \frac{1}{b_2 + \alpha b_1 r_1}\cdot\frac{\sqrt{L'_f}}{1-\sqrt{L'_f}}$$

Elution profile of the first component:

$$C_1 = \frac{1}{b_1 + b_2/(\alpha r_1)}\left(\sqrt{\frac{\gamma}{\alpha}\cdot\frac{t^0_{R,1} - t_0}{t - t_p - t_0}} - 1\right)$$

Elution profile of the second component:

$$C_2 = \frac{1}{b_2 + \alpha b_1 r_1}\left(\sqrt{\gamma\,\frac{t^0_{R,2} - t_0}{t - t_p - t_0}} - 1\right)$$

Time the mixed zone ends:

$$t_E = t_p + t_0 + \frac{\gamma}{\alpha}(t^0_{R,1} - t_0) = t_p + t_0\left(1 + \frac{\gamma Fa_1}{\alpha}\right)$$

Concentration of the second component at the end of the mixed zone:

$$C_2^B = \frac{\alpha - 1}{\alpha b_1 r_1 + b_2} = C^0_2 - \frac{C^0_1}{r_1}$$

(*Continued on p. 160*)

Table I *(Continued)*

Third zone: pure second component

Duration of the second component plateau:

$$\Delta t = t_I - t_E = Ft_0 \frac{\gamma}{\alpha}\left(a_2 \frac{\gamma}{\alpha} - a_1\right) = Fa_1 \cdot \frac{\gamma(\gamma - 1)}{\alpha} \cdot t_0$$

Time when the diffuse profile of the second component begins:

$$t_I = t_p + t_0\left[1 + \frac{Fa_2}{(1 + b_2 C_2^B)^2}\right] = t_p + t_0\left[1 + Fa_2\left(\frac{\gamma}{\alpha}\right)^2\right]$$

Diffuse profile of the pure second component:

$$C_2 = \frac{1}{b_2}\left(\sqrt{\frac{t_{R,2}^0 - t_0}{t - t_p - t_0}} - 1\right)$$

End of the elution profile:

$$t = t_p + t_{R,2}^0 = t_p + t_0(1 + Fa_2)$$

breakthrough curve (frontal analysis), and used in their model a differentia mass balance equation:

$$\frac{\partial C}{\partial t} + F \cdot \frac{\partial C_s}{\partial t} + u \cdot \frac{\partial C}{\partial z} = D_L \cdot \frac{\partial^2 C}{\partial t^2} \tag{46}$$

where D_L is the axial dispersion coefficient, and the solid film driving force model as the kinetic equation

$$\frac{\partial C_s}{\partial t} = k_m(q - C_s) \tag{47}$$

They have shown that with this model, and in the case of a breakthrough curve, the contributions of axial dispersion and of the mass transfer resistances are additive. There is an additional, second-order coupling term between the axial dispersion and the mass transfer resistance, but this coupling term is very small in most instances and can be ignored. However, unlike in linear chromatography, this additivity is concentration dependent and given by

$$H = \frac{2D_L}{u} + 2\left(\frac{k}{1 + k}\right)^2 \frac{u}{kk_m} \tag{48}$$

where H is the height equivalent to a theoretical plate, k is the slope of the isotherm chord, $k = F(\Delta q/\Delta C)$ and k_m is the lumped mass transfer coefficient, related to the film mass transfer coefficient, k_f, and the pore diffusion coefficient, D_p [21]. Eqn. 48 is very important. It proves that, at least in the case of frontal analysis and assuming the solid film linear driving force kinetics, the contribution of axial dispersion and mass transfer resistances are additive, as in linear chromatography. However, as k is concentration dependent, eqn. 48 shows that, in contrast to linear chromatography, the apparent dispersion coefficient in non-linear chromatography is concentration dependent. In linear chromatography, $k = k'_0$, and eqn. 48 reduces to the Van Deemter equation [22]:

$$H = \frac{2D_L}{u} + 2\left(\frac{k'_0}{1 + k'_0}\right)^2 \frac{u}{k'_0 k_m} \tag{49}$$

Eqn. 48 was derived for frontal analysis. In overloaded elution, we cannot apply either the equation derived for linear chromatography (eqn. 49) or that derived for frontal analysis (eqn. 48). We are of the opinion that, in overloaded elution, k should be replaced in eqn. 48 by the slope of the isotherm, $k = F(dq/dc) = k'_0/(1 + bC)^2$. Hence the situation in overloaded elution is more complicated than in the two previous cases since C, and hence k, vary along the elution band profile. We shall assume that D_a is independent of the concentration and that its value remains the same as obtained in linear chromatography. This is the essential approximation made when applying the equilibrium-dispersive model in non-linear chromatography. This approximation is an excellent one, as long

as the column efficiency is not very low (*i.e.*, exceeds a few hundred plates) [23].

4.2. Initial and boundary conditions

In order to solve eqn. 44, we need appropriate initial and boundary conditions. In overloaded elution, the initial condition is a column empty of the mixture components:

$$C_i(x, 0) = 0 \tag{50a}$$

The boundary condition is the injection of a rectangular pulse of duration t_p:

$$C_i(0, t) = C_i^0 \quad 0 < t \leq t_p \tag{50b}$$

$$C_i(0, t) = 0 \quad t > t_p \tag{50c}$$

The equilibrium-dispersive model can be used very conveniently for the study of other modes of chromatography, such as frontal analysis, displacement and gradient elution. It suffices to select the appropriate initial and boundary conditions which translate the experimental modes of operation of chromatography into mathematical conditions.

4.3. Adsorption isotherms

In order to solve eqn. 45a, we need the following parameters, characterizing the column design, column length, L, and cross-sectional area, and the column operating conditions, mobile phase flow-rate, F_v, and column dead volume. We also need the dispersion coefficients, $D_{a,i}$ and the equilibrium isotherms, $q_i(C_1, \ldots, C_i, \ldots)$. D_a can be calculated from eqn. 45b if we know the column HETP in linear chromatography. It is determined by measuring the variance of the Gaussian band profile obtained by injecting a very small amount of the compound of interest. However, the value of D_a obtained from eqn. 45b is valid for linear chromatography. As discussed above, we use the same value in the non-linear case. This is the approximation that permits the use of the equilibrium-dispersive model.

The last information which is needed is the adsorption isotherms $q_i(C_1, \ldots, C_i, \ldots)$, *i.e.*, the function relating the concentrations of the components in the stationary phase at equilibrium with the mobile phase.

4.3.1. Single-component isotherms

In the case of single components, the isotherm can be measured by frontal analysis (FA) [24,25], by elution by characteristic points (ECP) [26], by frontal analysis by characteristic points (FACP) [27] and by the retention time method (RTM) [15]. In many practical cases, it is observed that single-component adsorption data can be fitted reasonably well to the Langmuir isotherm:

$$q = \frac{aC}{1 + bC} \tag{51}$$

In some cases, the biLangmuir isotherm model [28]:

$$q = \frac{a_1 C}{1 + b_1 C} + \frac{a_2 C}{1 + b_2 C} \tag{52}$$

allows a considerable improvement of the fitting of the experimental data. This is the case, for example, with enantiomers for which there exist at least two distinct types of adsorption sites on a chiral stationary phase, the chiral selective sites and all the sites with which any kind of non-selective interactions can take place [29]. This is also the case with adsorption on heterogeneous surfaces. This model fits well the experimental data in many cases of adsorption of polar compounds on chemically bonded silica, on which unreacted silanols provide sites different from the bonded moieties.

Finally, the quadratic isotherm

$$q = \frac{q_s C(b_1 + 2b_2 C)}{1 + b_1 C + b_2 C^2} \tag{53}$$

provides a convenient isotherm to account for adsorption data that deviate markedly from the Langmuir model, and especially those isotherms which exhibit an inflection point.

4.3.2. Competitive multi-component isotherms

In overloaded chromatography, the feed components compete for access to the stationary phase, and as a result we need the competitive multi-component isotherms to account for the

band profiles in chromatography. The competitive isotherms can be obtained by one of two different approaches, one convenient and the other rigorous. We can measure the parameters of the single component isotherms of the various compounds involved by one of the methods mentioned above, and use these parameters in a proper multi-component isotherm model. This is highly convenient, provided that a suitable model is available. Otherwise, we have to measure directly the multi-component isotherms by frontal analysis of series of multi-component mixtures of various composition [30], or by recording the band profiles of a wide injection plug and applying the simple wave theory [31].

The competitive Langmuir isotherm is an extension of the single Langmuir isotherm:

$$q_i = \frac{a_i C_i}{1 + \sum_1^n b_j C_j} \tag{54}$$

The biLangmuir competitive isotherm is the sum of two competitive Langmuir isotherm terms [29]:

$$q_i = \frac{a_{i,1} C_i}{1 + \sum_1^n b_{j,1} C_j} + \frac{a_{i,2} C_i}{1 + \sum_1^n b_{j,2} C_j} \tag{55}$$

where the subscripts 1 and 2 refer to the adsorption sites 1 and 2, respectively.

The Langmuir competitive isotherm is the simplest model available to construct a competitive isotherm when single-component isotherms are available. However, it does not satisfy the Gibbs adsorption equation and, consequently, it is not consistent with thermodynamics, unless the column saturation capacities of the two components are the same [32]. This limits its usefulness to pairs of closely related isomers, *e.g.*, optical isomers [29].

In the case when the two single-component isotherms are different, the ideal adsorbed solution theory (IAS) provides a numerical procedure to calculate competitive isotherms. This method is based on the normalization of the spreading pressures [33]. The Levan–Vermeulen isotherm [34] is an attempt to correct the competitive Langmuir isotherm for its inconsistency in the case when each component follows a Langmuir isotherm, but the two column saturation capacities are different. By using the IAS concept and the Gibbs adsorption equation, Levan and Vermeulen [34] derived a binary competitive isotherm in the form of a rapidly converging expansion series which is easy to calculate and apply [35]. The Levan–Vermeulen isotherm reduces to the competitive Langmuir isotherm when the column saturation capacities of the two components are equal.

4.3.3. Role of the strong solvent in a mixed mobile phase

In principle, when we have a multi-component mixture and use as the mobile phase a multi-component solution, we have an n-component system (where n is the total number of mixture components and mobile phase constituents). Hence we need to write $n-1$ mass balance equations similar to eqn. 45a, and to solve these equations with a proper set of initial and boundary conditions (different for the mixture components and the mobile phase constituents), and using multi-component isotherms. The problem could easily acquire extreme complexity. We can simplify it greatly, however, because in liquid chromatography the absolute isotherm are meaningless.

Under certain conditions that we shall discuss later, we may assume that none of the constituents of the mobile phase adsorbs on the stationary phase. Using this assumption, we can determine the competitive isotherms of the feed components in equilibrium between the stationary phase and the solution considered as a pure solvent [36,37]. As a result, the mass balance equations for the mobile phase constituents can be ignored and only the mass balance equations for the feed components need to be solved. This assumption is valid in reversed-phase chromatography where the mobile phase modifiers are polar organic solvents which are weakly adsorbed by the stationary phase and do not compete strongly with the feed components for adsorption. In this mode of chromatography the organic modifier acts by increasing the mobile phase solubility of the feed components. In this

mode, this assumption gives excellent results in most practical cases [37].

The assumption that the mobile phase constituents do not adsorb on the stationary phase fails when the additive is adsorbed nearly as strongly as or more strongly than the feed components. Then the competition between the feed components and the mobile phase additives cannot be ignored. In this event, which is not infrequent in normal-phase chromatography where the mobile phase components control retention by competing with the sample components, the mass balance equations of the additives should be included in the system of mass balance equations to be solved, and the competitive isotherms of the components and the additives should be determined and used [38,39].

4.4. Analytical solution of the equilibrium dispersive model of a single component in a special case

There is no analytical solution of the equilibrium dispersive model. Attempts have been made to study the band profiles at the onset of column overloading, when the isotherm ceases to behave linearly and the influence of its curvature on the band profile begins to show. Houghton [40] and Haarhof and Van der Linde [41] have discussed this problem. An approximate solution is available, which replaces the isotherm by the first two terms of its Taylor expansion around the origin, *i.e.*, for a parabolic isotherm. It is valid for a moderate degree of column overloading.

If we assume that the isotherm can be written as

$$q = aC(1 - bC) \tag{56}$$

Then the solution obtained is [41]

$$X = \left| \frac{\exp(-\tau^2/2)}{\sqrt{2\pi}[\coth(m) + \mathrm{erf}(\tau\sqrt{2})]} \right| \tag{57}$$

where

$$X = |b|C \cdot \frac{k'_0}{1 + k'_0} \sqrt{N} \tag{58a}$$

$$m = N\left(\frac{k'_0}{1 + k'_0}\right)^2 L_f \tag{58b}$$

$$\tau = \frac{k'_0}{1 + k'_0} \cdot \sqrt{N} \cdot \frac{t - t_{R,0}}{t_{R,0} - t_0} \tag{58c}$$

The loading factor is defined as the ratio of the sample amount to the amount needed to saturate the column, an implicit reference to the Langmuir isotherm for which eqn. 56 is the two-term Taylor expansion. The loading factor is

$$L_f = \frac{n}{(1 - \epsilon)SLq_s} = \frac{nb}{\epsilon SLk'} = \frac{nb}{F_v(t_{R,0} - t_0)} \tag{59}$$

This solution is valid only for low values of the loading factor, because it assumes a parabolic isotherm. Actual isotherms will deviate rapidly from this assumption when the concentration increases. The range of validity of the solution depends also on the column efficiency. The results are excellent when $bC_M \leq 0.05$, where C_M is the maximum concentration of the band profile. The solution can still be used for $bC_M \leq 0.1$, as the error made in the band width remains smaller than 5% [42]. At higher column loadings the error increases significantly, because the parabolic isotherm deviates more and more from the actual isotherm (*i.e.*, a Langmuir isotherm) with increasing sample size.

4.5. Numerical solution of the equilibrium-dispersive model of chromatography

As in general there is no analytical solution of the equilibrium-dispersive model of chromatography, even in the single-component case, a numerical solution should be searched for. There are different approaches for obtaining such a numerical solution. The best method depends on the purpose of the calculation and the computer means available.

4.5.1. Orthogonal collocation method

The method of orthogonal collocation on finite elements [43,44] is one of the best methods to solve a set of partial differential equations such as eqn. 45, under the proper initial and boundary conditions and using the competitive equilibrium

isotherms. However, collocation methods have been developed for the solution of problems in the three-dimensional space, with complex geometries. In the case of a chromatographic column (one-dimensional space), these methods require long calculation time and it is difficult to adjust properly the parameters to obtain a stable numerical solution, as the conditions required have not been well defined. Nevertheless, several groups have derived the necessary computer programs and published profiles calculated by these methods.

4.5.2. Finite difference methods

The classical alternative approach for the solution of the set of eqns. 45 is the use of a finite difference method. Eqns. 45 can be rewritten as

$$\frac{\partial C}{\partial z} + \left\{ \frac{\partial \left[\frac{1}{u}(C + Fq) \right]}{\partial t} \right\} = \frac{D_a}{u} \cdot \frac{\partial^2 C}{\partial t^2} \qquad (60)$$

By letting $1/u(C + Fq)$ be G in eqn. 60, one obtains a simplified but equivalent equation:

$$\frac{\partial C}{\partial z} + \frac{\partial G(C)}{\partial t} = \frac{D_a}{u} \cdot \frac{\partial^2 C}{\partial t^2} \qquad (61)$$

In the finite difference method of solution of partial differential equations, each partial differential term is replaced by a forward, a backward or a central finite difference term. There are a large number of possible combinations for replacing the partial differential terms in eqn. 61 with various kinds and combinations of finite difference terms. However, the number of choices can be reduced dramatically by considering the facts that (i) the solution should be stable and (ii) the error term should be of second order with respect to the space and time increments, in order for the truncation or numerical error to be small enough and have a negligible influence on the solution. For example, if we use a central finite difference for the first term on the right-hand side of eqn. 61 and for the term on the left-hand side, and a backward finite difference term for the second term on the right-hand side, the following finite difference equation is obtained:

$$\frac{C_{n+1}^j - C_{n-1}^j}{2h} + \frac{G_n^{j+1} - G_n^j}{\tau} = \frac{D_a}{u} \cdot \frac{C_{n+1}^j - 2C_n^j - C_{n-1}^j}{h^2} \qquad (62)$$

where the subscript and n correspond to the space increments (h) and the superscripts and j to the time increments (τ). The error analysis of this calculation procedure shows that the error in this scheme is of the order of $O(\tau + h^2)$. Thus, the scheme introduces an error equivalent to a first-order partial differential term. Therefore, this procedure cannot be used, unless a very small value of the time increment, τ, can be selected. This would make the calculation too long. In linear chromatography an error of this type can be cancelled by adding an extra term exactly equivalent to the amount of the truncation error, but of opposite sign. This has been done by Lax and Wendroff [45]. The Lax and Wendroff scheme can be written as

$$\frac{C_{n+1}^j - C_{n-1}^j}{2h} + \frac{G_n^{j+1} - G_n^j}{\tau} = \left(\frac{D_a}{u} + \frac{\tau u_{z,0}}{2} \right) \frac{C_{n+1}^j - 2C_n^j - C_{n-1}^j}{h^2} \qquad (63)$$

Although this scheme gives an accurate solution in linear chromatography, it does not provide a very important contribution to the solution of this problem because we have an analytical solution for the equilibrium-dispersive model in linear chromatography. Eqn. 63 has been used by Lin and Guiochon [46] for the calculation of band profiles in non-linear chromatography. Serious difficulties are encountered in the choice of the integration increments to obtain a stable solution. Further, in non-linear chromatography, the truncation error is different from $\tau u_{z,0}/2$, and it is impossible to calculate it accurately. Therefore, the use of eqn. 63 introduces some error in non-linear chromatography, and we obtain only an approximate solution. The importance of the error is difficult to estimate exactly.

4.5.3. Replacing the axial dispersion term by a numerical dispersion

An alternative approach for writing a finite difference scheme of numerical integration of

eqns. 45 consists in ignoring the axial dispersion term in these equations and in compensating for it by adding a numerical dispersion. By ignoring the axial dispersion term, eqns. 45 become a first-order partial differential equation:

$$\frac{\partial C}{\partial z} + \frac{\partial G(C)}{\partial t} = 0 \tag{64}$$

The advantage of using eqn. 64 is that as it is a first-order partial differential equation, the stability condition and the error analysis are simple, at least with a linear isotherm. By replacing the partial difference terms in eqn. 64 with finite difference terms we make a numerical truncation error. This error can be analyzed and determined if we assume a linear isotherm. For a linear isotherm, by choosing the proper time and space increment, we can make the first-order numerical error exactly equal to the neglected axial dispersion term in eqn. 61 which has been ignored in eqn. 64. On the other hand, the error analysis is very difficult in non-linear chromatography. There are three possible schemes for this approach:

(i) The forward–backward differences [11,47, 48]:

$$C^j_{n+1} = C^j_n + \frac{h}{\tau}(G^j_n - G^{j-1}_n) \tag{65}$$

This numerical procedure has been found very attractive because of the fast execution by modern computers [48].

(ii) The backward–forward differences [48]:

$$G^{j+1}_n = G^j_n - \frac{\tau}{h}(C^j_n - C^j_{n-1}) \tag{66}$$

With this scheme, the concentration of the component at the new time position must be calculated from $G = C + Fq$, which requires an iteration procedure. This scheme is identical to the Craig model if we chose the time and space increments such that $h/r = u$.

(iii) The forward–backward$_{n+1}$ differences [49]:

$$\left(C + \frac{hG}{\tau}\right)^j_{n+1} = C^j_n + \frac{h}{\tau} G^{j-1}_{n+1} \tag{67}$$

With this scheme, the concentration, C, of the solute at the new space position must be calculated from $C + (h/\tau u)(C + Fq)$, which requires an iteration procedure.

Two types of problems are encountered when using this approach. First, it is impossible to determine the exact contribution of the numerical error in non-linear chromatography. We use the same condition as obtained in linear chromatography. This is an approximation, but a fairly good one, as the calculated band profiles are in excellent agreement with the experimental data. Second, we can choose only one value of the time and space increments for multi-component systems. The values of these increments can be determined only by equating the numerical dispersion coefficient with the axial dispersion coefficient for one of the components, or with the average axial dispersion coefficient of the mixture. This constitutes the second source of error in this approach. Its importance depends on the scheme selected and on the composition of the binary mixture studied.

The main advantages of this original approach for the calculation of numerical solutions of the equilibrium-dispersive model is that by using the proper time and space increments it is possible to obtain a stable solution and the calculation time is much shorter than with either of the other approaches. This advantage is of particular value for the first scheme (forward–backward difference).

4.6. Practical value of the equilibrium-dispersive model

Numerical calculation of solutions of the equilibrium-dispersive model in linear chromatography presents no difficulties, either theoretical or practical. When the model is applied to non-linear chromatography, a number of problems have to be solved.

From the fundamental viewpoint, the only serious difficulty is that we have shown that it is certainly impossible to obtain an exact solution of the equilibrium-dispersive model, because D_a is concentration dependent. On the other hand, in order to obtain easily a numerical solution of

this model, it is necessary to assume that D_a is independent of the concentration. If we assume that D_a is constant, however, we still obtain solutions that are satisfactory in practice, because the variation of D_a is not very important in the concentration range used in chromatography and the influence of D_a on the band profile is small compared with the determining influence of thermodynamics.

From a more practical viewpoint, the selection of a calculation method, we can use methods based on collocation one finite elements. These methods give satisfactory results but are slow and require significant amounts of CPU time. If we apply the Lax–Wendroff approach to a problem of non-linear chromatography, a source of error appears, because the truncation error in the non-linear case cannot be calculated, and we have to assume it to be the same as in the linear case. This method should be rejected for its lack of numerical stability.

If we apply the third approach, ignoring the axial dispersion term and compensating for it by the proper amount of numerical error, we find two main sources of error. First, the truncation error in the non-linear case cannot be calculated, and we have to assume that it is the same as in the linear case. Second, as the apparent dispersion term is compensated for by the numerical dispersion term, the calculation can be made with only one value of the apparent dispersion coefficient. In spite of these approximations, however, the calculated band profiles are very close to the experimental band profiles, because at low concentrations the effect of the axial dispersion is accounted for accurately, whereas at high concentrations the effect of the axial dispersion becomes small compared with the influence of the thermodynamics on these profiles.

5. COMPARISON OF CALCULATED BAND PROFILES AND EXPERIMENTAL RESULTS

In order to calculate the experimental band profiles, we need the following experimental conditions: adsorption isotherm; sample size; mobile phase flow-rate; column dimensions; column hold-up time; and HETP under linear conditions. The column HETP can be obtained easily by injecting a very small amount of sample and measuring the band width. It is a function of the mobile phase velocity. The column dimensions, mobile phase velocity, hold-up volume and sample size are easily measured.

However, the band profile under overloaded conditions is very sensitive to the adsorption isotherm. These equilibrium isotherms have to be measured accurately in order to achieve good agreement between theoretical and experimental profiles. This is often what limits the usefulness of a model that could otherwise permit accurate band profile prediction. Too little is known yet about competitive isotherms.

5.1. Calculated and experimental band profiles in the case of single-component bands

We compare in Figs. 4 and 5 [37] experimental band profiles (symbols) with the results of calculations for normal- and reversed-phase chromatography (solid lines). Fig. 4 corresponds to acetophenone on a silica column eluted with *n*-hexane–ethyl acetate (97.5:2.5). Fig. 5 corresponds to phenol on a C_{18} chemically bonded silica column eluted with methanol–water

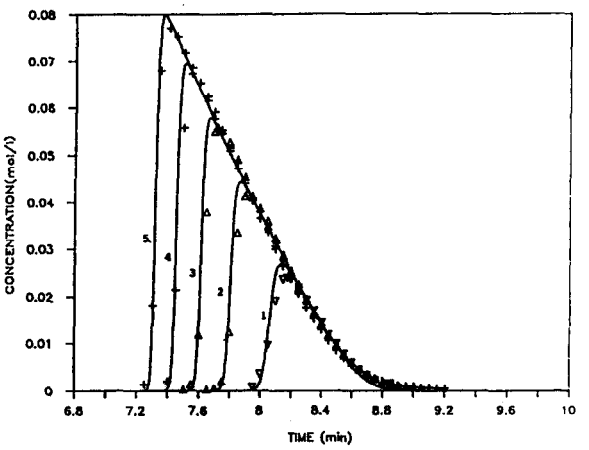

Fig. 4. Comparison of the calculated (solid lines) and the experimental (symbols) band profiles of acetophenone on silica. Mobile phase: ethyl acetate–*n*-hexane (2.5:97.5). L = 25 cm; d = 4.6 mm; F_v = 2 ml/min; N = 5000. Sample sizes: 1 = 0.025; 2 = 0.05; 3 = 0.075; 4 = 0.1; 5 = 0.125 mmol. From ref. 37 (© American Chemical Society).

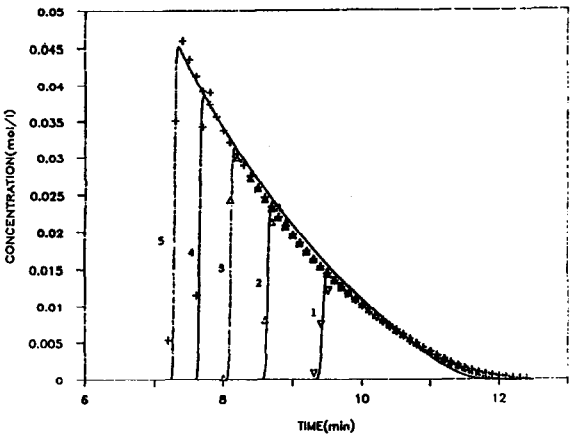

Fig. 5. Comparison of the calculated (solid line) and experimental (symbols) band profiles of phenol on octadecyl chemically bonded silica. Mobile phase: methanol–water (20:80). $L = 25$ cm; $d = 4.6$ mm; $F_v = 1$ ml/min; $N = 5000$. Sample sizes: 1 = 0.015; 2 = 0.03; 3 = 0.045; 4 = 0.06; 5 = 0.075 mmol. From ref. 37 (© American Chemical Society).

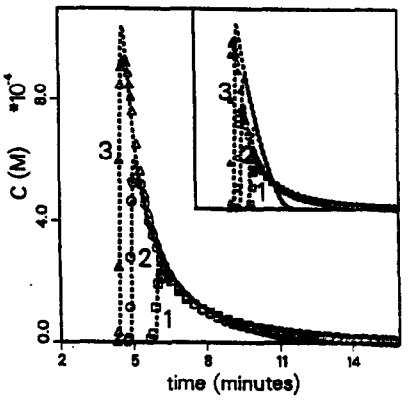

Fig. 6. Comparison of the calculated (solid line) and experimental (symbols) band profiles of N-benzoyl-L-phenylalanine on a Resolvosil-BSA-7 column. Mobile phase: 0.1 *M* aqueous phosphate buffer solution (pH 6.8) with containing 7% (v/v) of 1-propanol. $L = 15$ cm; $d = 4$ mm; $F_v = 1$ ml/min; $N = 700$. Sample size: 1 = 0.494; 2 = 0.989; 3 = 1.48 μmol. BiLangmuir isotherm: selective site $a_1 = 20.1$, $q_{s,1} = 0.000556$ mol/l; non-selective site, $a_2 = 7.09$, $q_{s,2} = 0.217$ mol/l. From ref. 29 (© American Institute of Chemical Engineers).

(20:80). In both instances there is very good agreement between theory and experiments. However, it must be emphasized that in each instance the isotherm was measured with the same column as used for the determination of the overloaded band profiles and fitted to a Langmuir isotherm. The use of the ECP method should be avoided in the comparison between experimental and calculated band profiles, as it is easy to fall into a circular argument. For practical applications, however, the ECP method often provides excellent adsorption data.

In the previous cases, the experimental data obtained in the determination of the single-component isotherms were fitted correctly to the Langmuir equation (eqn. 51). In the case of the results shown in Fig. 6, a biLangmuir isotherm was needed. For enantiomers on chiral selective stationary phases, a minimum of two different types of sites exist on the surface. One type of sites is enantioselective whereas the other is not [29]. For mandelic acid on immobilized bovine serum albumin (BSA), the use of a biLangmuir isotherm permitted the achievement of excellent simulations of the experimental bands.

We compare in Fig. 7 experimental and calculated band profiles for dodecylbenzene on graphitized carbon [50,51]. The behavior of

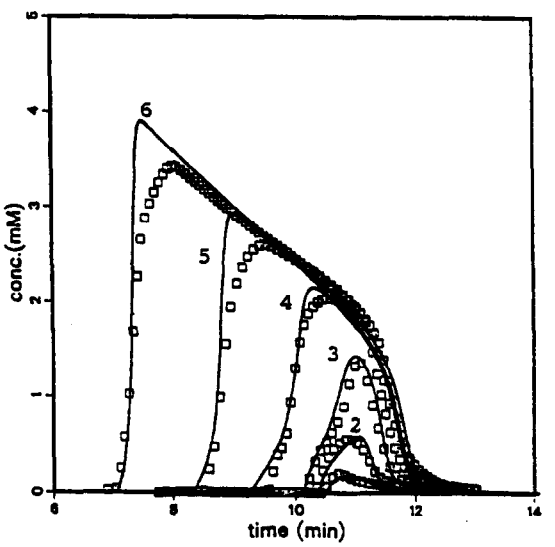

Fig. 7. Comparison of the calculated (solid lines) and experimental (symbols) elution profiles of phenyldodecane for different masses injected [49]. Isotherm model in eqn. 68. Experimental conditions: column packed with graphitized carbon, $L = 15$ cm, I.D. = 0.46 cm; mobile phase, acetonitrile; temperature, 50°C; mobile phase flow-rate, 1 ml/min; sample concentration, 67 m*M*. Sample volumes: 1 = 5; 2 = 10; 3 = 20; 4 = 50; 5 = 100; 6 = 180 μl. From ref. 51 (© American Chemical Society).

carbon as an adsorbent in liquid chromatography is very different from that of silica and chemically bonded silica. It presents a strong affinity for alkyl chains and contains a certain amount of high-energy sites selective of these chains. Further, adsorbate–adsorbate interactions are especially strong between alkyl chains sorbed on graphitized carbon, on the surface of which they lie flat and parallel. The result is an adsorption isotherm that is convex downwards. The two phenomena combine to give a composite adsorption isotherm with the equation

$$q = \frac{q_{s,1}C(b_1 + 2b_2C)}{1 + b_1C + b_2C^2} + \frac{q_{s,2}b_3C}{1 + b_3C} \quad (68)$$

Adsorption data and band profiles are in excellent agreement with the model and the results of calculation performed with the model.

5.2. Comparison of calculated band profiles with experimental results in the case of multi-component bands

A new difficulty arises when we try to compare experimental and calculated band profiles. With multi-component systems, and when the column is overloaded to the extent that the bands of the two components of the binary mixture overlap, the direct determination of the individual band profiles from the detector response is not possible in general. It is exceptional that two compounds whose interference on a column is not accidental have UV spectra that are different enough to permit the accurate detection of one of them in the presence of the other. In the few reported cases where the band profile of a component is determined from the detector response on a frequency where the other does not absorb, the separation was purely academic. In order to determine the individual profiles, fractions must be collected at sufficiently close intervals and analyzed in order to find the composition of the eluent as a function of time [29,52].

We note that, unless the detector has the same response factor for the two components, it is also not possible to determine the total concentration profile from the chromatogram. When the detector response is not linear, the deconvolution of the detector response is a complex problem. A notable and useful exception is enantiomers for which the detector usually provides the total concentration profile by simple calibration with the racemic mixture or one of the enantiomers.

The competitive isotherms are necessary for the calculation of the individual band profiles. Whereas in the single-component case the Langmuir model is often a reasonable first approximation, the competitive isotherms rarely follow the competitive Langmuir isotherm model. The only exception that we have found concerns enantiomers on immobilized BSA. The reason for this success of the Langmuir model stems from the characteristics of the retention mechanisms involved. We have two very similar components, which behave in identical ways for anything but the enantioselective mechanism. This mechanism involves the adsorption of the molecules in a pouch of the BSA molecule, thus effectively shielding them, and avoiding any adsorbate–adsorbate interactions. For this mechanism, the column saturation capacities of the two components are identical, so the Langmuir model is thermodynamically sound. Further, the common column saturation capacity for the active sites is low. Thus, the column becomes overloaded with small sample amounts. Because adsorption needs be measured in a low range of concentrations, the liquid and adsorbed phases are close to ideal, and the conditions required for the validity of the Langmuir isotherm are nearly fulfilled. As a result, in most instances of separation of optical isomers we have studied so far, the band profiles of the enantiomers are well accounted for by using a bilangmuir competitive isotherm model, whose parameters are those obtained by single-component isotherm measurement [24,53].

We show in Figs. 8–10 a series of experimental band profiles and the profiles calculated using a backward-forward finite difference scheme (eqn. 66). The components studied were N-benzoyl-D- and -L-alanine [53]. The single-component isotherms of each of these optical isomers was measured on the same column. These experimental data were well fitted by a bilangmuir isotherm. A bilangmuir competitive isotherm

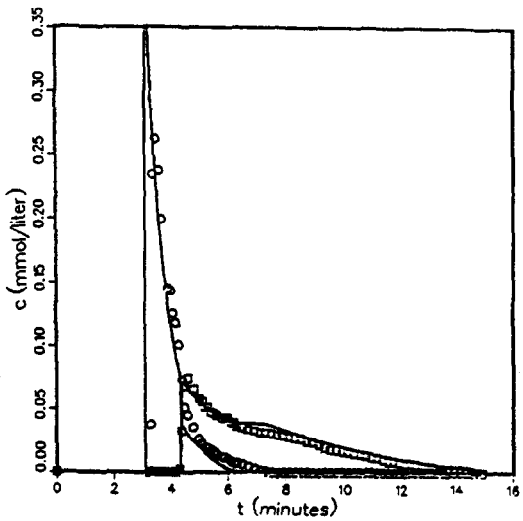

Fig. 8. Comparison of the calculated (solid line) and experimental (symbols) individual band profiles for a racemic mixture of N-benzoyl-L- (○) and -D-phenylalanine (□) on a Resolvosil-BSA-7 column. Conditions as in Fig. 7, except the mobile phase was a 10 m*M* aqueous phosphate buffer solution (pH 6.7) containing 3% (v/v) of 1-propanol. Samples sizes: 0.26 μmol for each isomer. Binary competitive Langmuir isotherm: selective site, $a_{1,L} = 14.16$, $a_{1,D} = 35.09$, $q_{s,1,L} = 0.0019$ mol/l, $q_{s,1,D} = 0.0020$ mol/l; non-selective site, $a_2 = 4.41$, $q_{s,2} = 0.01995$ mol/l. From ref. 53 (© the American Chemical Society).

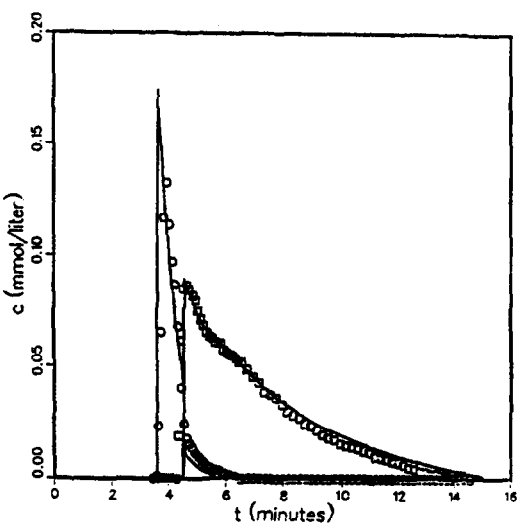

Fig. 9. Same comparison as in Fig. 8, except 1:3 mixture; sample size, 0.105 μmol of L- and 0.392 μmol of D-isomer. From ref. 53 (© American Chemical Society).

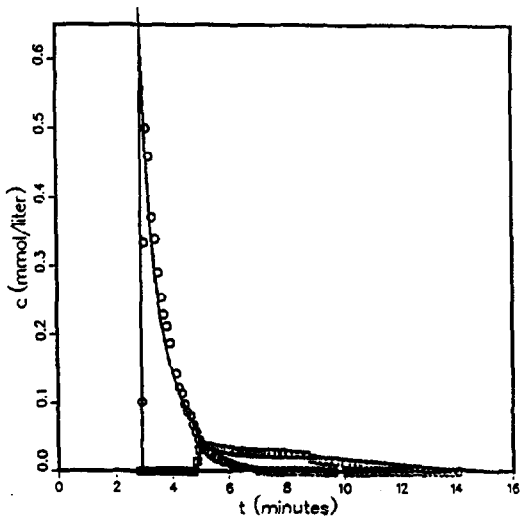

Fig. 10. Same comparison as in Fig. 8, except 3:1 mixture; sample size, 0.491 μmol of L- and 0.165 μmol of D-isomer. From ref. 53 (© American Chemical Society).

using these coefficients was used for the calculation of the band profiles. In all three figures, the solid lines represent the results of calculations and the symbols (circles for the L-isomer, squares for the D-isomer) are the experimental data. There is a very good agreement in all instances between the calculated and experimental profiles. Fig. 8 compares the bands of the two enantiomers for a racemic mixture. The displacement and the tag-along effects can be seen in these bands. Fig. 9 compares the bands of the isomers in a 1:3 mixture. As predicted by theory, the intensity of the displacement of the first component by the second increases with increasing relative concentration of the second component (compare Figs. 8 and 9). Fig. 10 compares the bands of the two isomers in a 3:1 mixture. As predicted by theory, the intensity of the tag-along effects increases with increasing ratio of the concentrations of the first and second components.

Finally, we show in Fig. 11 a comparison between experimental and calculated profiles for 2-phenylethanol and 3-phenylpropanol [54]. The single-component isotherms follow the Langmuir model, but the competitive isotherms are not well accounted for by the competitive Langmuir

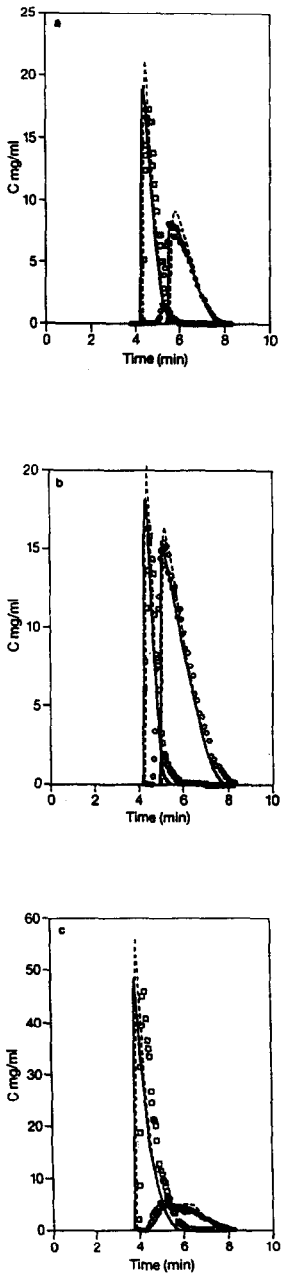

Fig. 11. Comparison of the profiles calculated with the forward–backward difference (eqn. 65), using the actual injection profile (solid lines) and a rectangular pulse injection (dashed line), and the experimental (symbols) elution profiles of a mixture of 2-phenylethanol and 3-phenylpropanol. Experimental conditions: column, 25 cm × 0.46 cm I.D., packed with 10-μm Vydac C_{18}; mobile phase, methanol–water; flow-rate, 1 ml/min. Sample sizes: 10 + 10 mg (L_f = 7 and 7%); (b) 7 + 21 mg (L_f = 5 and 15%); (c) 30 + 10 mg (L_f = 21 and 7%). From ref. 54.

model. The band profiles predicted are in reasonable agreement with the experimental profiles, but significant, systematic differences are obvious. This illustrates the need for a good competitive isotherm model for the accurate prediction of band profiles.

6. CONCLUSIONS

The ideal model gives an excellent idea of the phenomena that take place during a chromatographic separation. The understanding of the chromatograms derived from the ideal model provides a profound insight into what is happening during the progressive disentanglement of the component bands. Particularly among scientists coming to preparative chromatography from the field of analytical chemistry, the didactic value of the ideal model cannot be overestimated.

In all cases of practical importance in preparative chromatography, the equilibrium-dispersive model offers an accurate and rapid procedure for calculating the individual band profiles, provided that the equilibrium isotherms are available. This is because materials scientists have succeeded in manufacturing particles of stationary phases through which mass transfers proceed rapidly, and on the surface of which the kinetics of adsorption–desorption are fast. It is exceptional that a chromatographic separation has to be conducted with packing material giving a column with less than a few tens of theoretical plates. Then the production rate would be very poor. Excellent calculation procedures are available for this model, making easily accessible to chemical engineers the simulation of preparative chromatography. Further, as chromatogram simulation becomes easy, the computer optimization of the design and operating parameters of a separation is now accessible. Using this approach, we have been able recently to calculate the production rate and the recovery yield of a component at a given degree of purity, under a variety of simulated experimental conditions. The experimental data obtained independently agree to within 5–8% with the calculated values [55–57].

REFERENCES

1 S. Golshan-Shirazi and G. Guiochon, in F. Dondi and G. Guiochon (Editors), *Theoretical Advancement in Chromatography and Related Separation Techniques*, Kluwer, Dordrecht, 1992, p. 1.
2 Q. Yu and N.-H.L. Wang, *Comput. Chem. Eng.*, 13 (1989) 915.
3 R.D. Whitley, K.E. Van Cott, J.A. Berninger and N.-H.L. Wang, *AIChE J.*, 37 (1991) 555.
4 J.N. Wilson, *J. Am. Chem. Soc.*, 62 (1940) 1583.
5 D. DeVault, *J. Am. Chem. Soc.*, 65 (1943) 532.
6 A.C. Offord and J. Weiss, *Nature*, 155 (1945) 725.
7 E. Glueckauf, *Proc. R. Soc. London, Ser A*, 186 (1946) 35.
8 E. Glueckauf, *J. Chem. Soc.*, (1947) 1302.
9 H.K. Rhee, R. Aris and N.R. Amundson, *Trans. R. Soc. London, Ser. A*, 267 (1970) 419.
10 F. Helfferich and G. Klein, *Multicomponent Chromatography. A Theory of Interferences*, Marcel Dekker, New York, 1970.
11 G. Guiochon and L. Jacob, *Chromatogr. Rev.*, 14 (1971) 77.
12 S. Golshan-Shirazi and G. Guiochon, *J. Phys. Chem.*, 93 (1989) 4143.
13 S. Golshan-Shirazi and G. Guiochon, *J. Phys. Chem.*, 94 (1990) 495.
14 S. Golshan-Shirazi and G. Guiochon, *Anal. Chem.*, 60 (1988) 2364.
15 S. Golshan-Shirazi and G. Guiochon, *Anal. Chem.*, 61 (1989) 462.
16 S. Golshan-Shirazi and G. Guiochon, *J. Chromatogr.*, 484 (1989) 125.
17 R. Aris and N.R. Amundson, *Mathematical Methods in Chemical Engineering*, Prentice Hall, Englewood Cliffs, NJ, 1st ed., 1973.
18 E. Glueckauf, *Ion-Exchange and Its Applications*, Metcalfe and Cooper, London, 1955, p. 34.
19 E.V. Dose and G. Guiochon, *Anal. Chem.*, 62 (1990) 1723.
20 H.K. Rhee and N.R. Amundson, *Chem. Eng. Sci.*, 27 (1972) 199.
21 E. Glueckauf, *Trans. Faraday Soc.*, 51 (1955) 1540.
22 J.J. Van Deemter, F.J. Zuiderweg and A. Klinkenberg, *Chem. Eng. Sci.*, 5 (1956) 271.
23 S. Golshan-Shirazi and G. Guiochon, in preparation.
24 D.H. James and C.S.G. Phillips, *J. Chem. Soc.*, (1954) 1066.
25 G. Schay and G. Szekely, *Acta Chim. Hung.*, 5 (1954) 167.
26 E. Cremer and J.F.K. Huber, *Angew. Chem.*, 73 (1961) 461.
27 E. Glueckauf, *Trans. Faraday Soc.*, 51 (1955) 1540.
28 D. Graham, *J. Phys. Chem.*, 57 (1953) 665.
29 S. Jacobson, S. Golshan-Shirazi and G. Guiochon, *AIChE J.*, 37 (1991) 836.
30 J.M. Jacobson, J.H. Frenz and Cs. Horváth, *Ind. Eng. Chem. Res.*, 26 (1987) 43.
31 Z. Ma, A.M. Katti and G. Guiochon, *J. Phys. Chem.*, 94 (1990) 6911.
32 C. Kembell, E.K. Rideal and E.A. Guddenheim, *Trans. Faraday Soc.*, 44 (1948) 948.
33 A.L. Myers, and J.M. Prausnitz, *AIChE J.*, 11 (1965) 121.
34 M.D. Levan and T. Vermeulen, *J. Phys. Chem.*, 85 (1981) 3247.
35 S. Golshan-Shirazi, J.-X. Huang and G. Guiochon, *Anal. Chem.*, 63 (1991) 1147.
36 E. sz. Kováts, in F. Bruner (Editor), *The Science of Chromatography (Journal of Chromatography Library*, Vol. 32), Elsevier, Amsterdam, 1985, p. 205.
37 S. Golshan-Shirazi and G. Guiochon, *Anal. Chem.*, 60 (1988) 2634.
38 S. Golshan-Shirazi and G. Guiochon, *J. Chromatogr.*, 461 (1989) 1.
39 S. Golshan-Shirazi and G. Guiochon, *J. Chromatogr.*, 461 (1989) 19.
40 G. Houghton, *J. Phys. Chem.*, 67 (1963) 84.
41 P.C. Haarhof and H.J. van der Linde, *Anal. Chem.*, 38 (1966) 573.
42 S. Golshan-Shirazi and G. Guiochon, *J. Chromatogr.*, 506 (1990) 495.
43 Q. Yu and N.-H.L. Wang, *Comput. Chem. Eng.*, 13 (1989) 915.
44 Z. Ma and G. Guiochon, *Comput. Chem. Eng.*, 15 (1991) 415.
45 P.D. Lax and B. Wendroff, *Commun. Pure Applied Math.*, 13 (1960) 217.
46 B.C. Lin and G. Guiochon, *Sep. Sci. Technol.*, 24 (1989) 809.
47 G. Guiochon, S. Golshan-Shirazi and A. Jaulmes, *Anal. Chem.*, 60 (1988) 1856.
48 M. Czok and G. Guiochon, *Comput. Chem. Eng.*, 14 (1990) 1435.
49 B.C. Lin, S. Golshan-Shirazi, Z. Ma and G. Guiochon, *Anal. Chem.*, 60 (1988) 2647.
50 M. Diack and G. Guiochon, *Anal. Chem.*, 63 (1991) 2608.
51 A.M. Katti, M. Diack, M.Z. El Fallah, S. Golshan-Shirazi, S.C. Jacobson, A. Seidel-Morgenstern and G. Guiochon, *Acc. Chem. Res.*, 25 (1992) 366.
52 A.M. Katti and G. Guiochon, *J. Chromatogr.*, 499 (1990) 21.
53 S. Jacobson, S. Golshan-Shirazi and G. Guiochon, *J. Am. Chem. Soc.*, 112 (1990) 6492.
54 A.M. Katti, M. Czok and G. Guiochon, *J. Chromatogr.*, 556 (1991) 205–218.
55 A. Felinger and G. Guiochon, *J. Chromatogr.*, 591 (1992) 31.
56 S.C. Jacobson, A. Felinger and G. Guiochon, *Biotechnol. Prog.* 8 (1993) 533.
57 S.C. Jacobson, A. Felinger and G. Guiochon, *Biotechnol. Bioeng.*, 40 (1993) 1210.